Force fabric and macroscopic friction in two-dimensional granular materials

Ernesto Medina,[1] Xavier García,[1] and Vanessa Urdaneta[1,2]
[1]*Laboratorio de Física Estadística de Sistemas Desordenados, Centro de Física, Instituto Venezolano de Investigaciones Científicas (IVIC), Apartado 21827, Caracas 1020 A, Venezuela*
[2]*Departamento de Ciencias de la Tierra, Universidad Simón Bolívar, Apartado 89000, Caracas 1080A, Venezuela*
(Received 16 November 2009; published 19 February 2010)

We study the relationship between the local grain-grain friction and the force texture in a granular pile to its macroscopic emergent frictional values. We account for the force geometrical properties by a model that assumes the existence of slide planes that define macroscopic friction angles. The model depends on the measured angular distribution of contact forces and a single parameter, to be fitted, that is a function of the roughness of the slide plane. The model is tested by a state-of-the-art model of a two-dimensional granular pile built by depositing grains under gravity and submitted to an external uniaxial stress.

DOI: 10.1103/PhysRevE.81.022301 PACS number(s): 45.70.Cc, 46.55.+d

The behavior of granular materials under loading has been a subject of strong recent interest since it reveals many of the unique mechanical features of this phase of matter. Many of these features are inherited by granular rocks under uniaxial loading and the anisotropic stresses developed under these conditions determine their mechanical strength and behavior under shear. Mechanical features of composite materials such as sedimentary rocks are commonly studied as macroscopic quantities with little regard of the geometrical configurations and the local system components. Mechanical yield is understood as the resulting phenomena when forces overcome the Coulomb condition [1]. Although this criterion involves some of the essential physics, it is not fully applicable in granular systems in which processes such as dilatancy, stress-induced anisotropy, and contact force networks are ubiquitous [2].

Approaches that regard local details [3] and granular elasticity theories provide more detailed explanations of the macroscopic behavior of composite materials, including nonlinear elastic relations [2,4]. Nevertheless, those approaches do not yet fully reconcile the macroscopic or effective observations with the microscopic structure and physical properties of the system elements. In contrast to the behavior of a classical gas of particles, where only long-wavelength excitations determine the thermodynamic behavior, in granular material, there always remains a reference to the local length scale behavior.

Here we study the relation between the intergranular friction and the macroscopic friction as derived from the Mohr-Coulomb circles of a compacted two-dimensional (2D) sample. The latter case has been analyzed experimentally in Ref. [5], where a connection is made between the microscopic friction and macroscopic friction from the Rankine analysis. Nevertheless, in this work, the local orientation of forces was only surmised, so various plausible scenarios were proposed. A related study of the geometrical effects on macroscopic friction is that of Ref. [6] where, as in [5], a local friction angle can be defined by the ratio of the local tangential and normal forces.

A simple 2D model can give us insight into the relation between the local force fabric or configuration of forces between grains and the macroscopic behavior of the pile. In Refs. [5,6], the authors related the normal and tangential forces applied to a plane in the material (macroscopic description) to the normal and tangential forces between grains composing that plane. Following Eber [5], we can relate τ and σ as depicted in Fig. 1 on a particular plane, to the local grain-grain forces by

$$\mu_m = \frac{\tau \cos\gamma + \sigma \sin\gamma}{\sigma \cos\gamma - \tau \sin\gamma}, \tag{1}$$

where μ_m is the local microscopic friction, γ, as defined in Fig. 1, is the angle between the normal force between grains, and δ is the range of angles over which γ can vary. The macroscopic friction is given by $\mu_M = \tau/\sigma = \tan\varphi_M$, so we can write

$$\mu_m = \tan\varphi_m = \frac{\tan\varphi_M \cos\gamma + \sin\gamma}{\cos\gamma - \tan\varphi_M \sin\gamma}. \tag{2}$$

Solving for $\tan\varphi_M$, we arrive at

$$\tan\varphi_M = \frac{\tan\varphi_m - \tan\gamma}{1 + \tan\gamma\tan\varphi_m} = \tan(\varphi_m - \gamma). \tag{3}$$

As can be seen from the previous equation, the angle γ is referred to the principal plane that defines σ and τ so that such an angle depends on φ_M itself. Referring to Fig. 2, we can derive the relation

$$\tan\varphi_M = \tan\left(\frac{2}{3}[\varphi_m - \varphi + \pi/4]\right). \tag{4}$$

The right-hand side of this equation only depends on the microscopic friction angle φ_m and the angle φ giving the orientation of the contact with respect to the vertical axis (see Fig. 2) of the sample. In order to obtain the macro friction angle, one must now introduce information on the distribution of the φ that is given by the texture. The texture distribution is determined directly from the simulation so that one can directly obtain

$$\langle\mu_M\rangle = \int_{\varphi_{min}}^{\varphi_{max}} P(\varphi)\tan\left(\frac{2}{3}[\varphi_m - \varphi + \pi/4]\right)d\varphi, \tag{5}$$

where $P(\varphi)$ gives the distribution of orientations of the forces between individual grains. The limit angles $\varphi_{min}, \varphi_{max}$

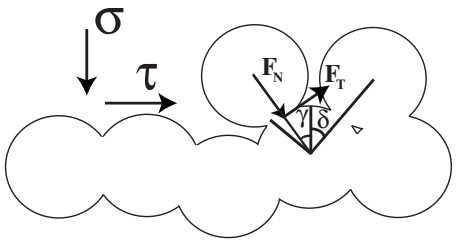

FIG. 1. Bottom of a slide line for a two-dimensional granular model defining the Mohr circle τ and σ pair in relation to the local tangential F_T and normal F_N forces between the grains as proposed by Eber [5].

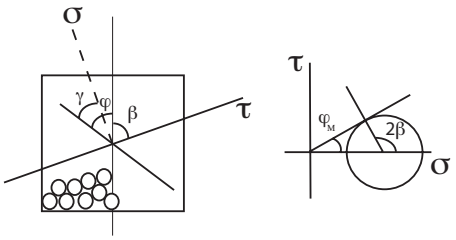

FIG. 2. Convention for angle γ measured from the plane defined by the Mohr construction (τ,σ), and φ measured from the principal direction. Angle β is depicted and related to the inclination of the plane identifying the macroscopic failure angle φ_M.

are critical in making sense of this relation. We have the restriction of $\tan \phi_M > 0$, so that $\varphi \leq \varphi_m + \pi/4$. The upper limit can be derived from the condition that the argument of the tangent does not exceed $\pi/2$, where the tangent changes sign. Nevertheless, the lower limit depends on the structure of the sliding plane [7] and is further restricted. For a perfectly ordered straight line of spheres of the same size, the lower limit is $-\pi/6$. Roughness of such a plane (line for a two-dimensional pack) will yield larger average angles [5].

In order to test the previous model, we proceed to simulate a detailed two-dimensional granular model. Very accurate representations of unconsolidated sands have been developed in two and three dimensions [8] that consider a nonlinear Hertz-Mindlin model for the grain-grain interactions and also account for surface elasticity [9,10]. At the microscopic level, the grains interact with a repulsive nonlinear viscoelastic force [8–10] $\mathbf{F}_c$ given by

$$\mathbf{F}_c = \{\sqrt{\xi_n R_f}(\kappa_n \xi_n - \gamma_n \dot{\xi}_n)\}\hat{\mathbf{n}} + \mathbf{F}_s, \tag{6}$$

where first term represents the force $\mathbf{F}_n$ normal to the contact area. For the labeled grains 1 and 2 with radii R_1, R_2 and positions $\mathbf{r}_1$, $\mathbf{r}_2$, $\xi_n = \max(0, R_1 + R_2 - |\mathbf{r}_2 - \mathbf{r}_1|)$ and $\hat{\mathbf{n}} = (\mathbf{r}_1 - \mathbf{r}_2)/|\mathbf{r}_1 - \mathbf{r}_2|$ is the unitary vector joining the grains centers. The normal stiffness of the contact $\kappa_n = 4G/(1-\nu)$, where $G = 29$ GPa is the shear modulus and $\nu = 0.08$ is the Poisson coefficient, $R_f = (R_1 R_2)/(R_1 + R_2)$ is an effective radius, and $\sqrt{\xi_n R_f}$ is the radius of contact area. The second term in braces in Eq. (6) represents the viscous forces for normal deformations, where γ_n is a damping constant set here to 2.3×10^{-6} gr/(cm s).

The shear force in Eq. (6),

$$\mathbf{F}_s = -\min[\sqrt{\xi_n R_f}(\kappa_s \vec{\xi}_s - \gamma_s \dot{\vec{\xi}}_s), \mu_m |F_n| \hat{s}], \tag{7}$$

depends on contact history and cannot be determined by the position of grains. The tangential stiffness is $\kappa_s = 8G/(2-\nu)$ and μ_m represents the Coulomb friction coefficient. The term $\gamma_s = 2.0 \times 10^{-6}$ gr/(cm s) is a damping coefficient and $\xi_s = \int_0^t \dot{\xi}_s(t')dt'$ is the tangential displacement that took place since the contact was first established. $\dot{\vec{\xi}}$ is the relative velocity, of the grain surfaces, $\dot{\vec{\xi}}_s = \dot{\vec{\xi}} - (\dot{\vec{\xi}} \cdot \hat{n})\hat{n}$, and $\hat{s} = \dot{\vec{\xi}}_s / |\dot{\vec{\xi}}_s|$. The vector $\vec{\xi}_s$ can be computed from the relative displacement vector $\mathbf{d}$ between the grains in contact as $\vec{\xi}_s = \mathbf{d} - (\mathbf{d} \cdot \hat{\mathbf{n}}_0)\hat{\mathbf{n}}_0$, with $\hat{\mathbf{n}}_0$ the normal of the contact when it is created. Whenever a contact is established for the first time, the viscoelastic part of Eq. (7) (left term) is activated and the grains feel a force opposed to the tangential displacement. Upon exceeding the threshold of Coulomb dry friction, sliding occurs following the frictional term (right term) and the elastic spring is broken. When the tangential velocity drops to zero or is inverted, the elastic spring is reactivated with zero elongation, and the friction force is turned off [11].

An initial pack is constructed following a ballistic algorithm that models the settling of the grains under gravity [11]. Periodic boundary conditions are imposed in the direction $\hat{x}$ perpendicular to the gravity. The diameter R of each grain is chosen at random from a flat distribution in the range of 0.01–0.03 cm. The method produced an initial condition of porosity $\approx 17.7\%$ and marginal grain-to-grain overlaps. About 10^4 disks were packed in a rectangular box of size 58×74 in units of the maximum grain diameter (see Fig. 3).

Once the initial sample was constructed, the intergranular friction is turned on and set to a different value in the range $\mu_m \approx 0.1 - 0.7$ in each of eight different simulations where the samples are cyclicly compressed. The compaction cycles are

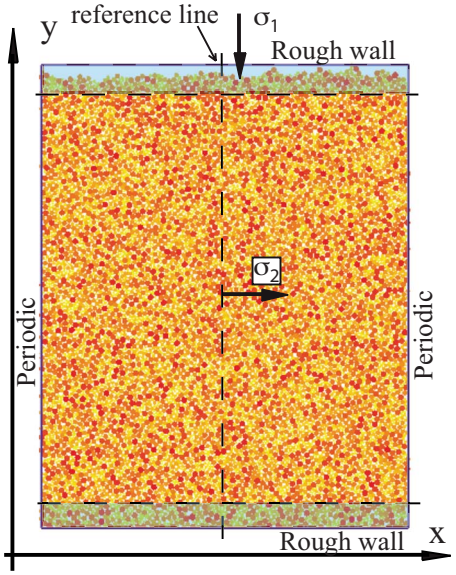

FIG. 3. (Color online) A simulation cell with 10 000 grains taken from a narrow distribution of sizes as described in the text. σ_1 denotes the vertical stress while lateral stress is measured by σ_2. The lateral conditions are periodic and the top and bottom walls have friction so that slip of the granular pack is avoided.

performed by imposing macroscopic strained states on the sample. Two rough walls are implemented by freezing the grains in slabs of four maximum grain diameters at each of the extremes of the y axis of the sample. Each strained state is then reached by moving the rough walls in the vertical direction $\hat{y}$ by a finite amount and then leaving ample time for the system to relax the kinetic energy and the stress accumulated near the walls. The walls move toward the sample core for a compaction or in the opposite direction during decompaction.

The vertical stress σ_1 is computed as the average force on the walls divided by the sample width in the direction perpendicular to the compaction $\hat{x}$. To compute the lateral stress, an imaginary line is drawn parallel to the $\hat{y}$ axis and passing through the sample center. The stress σ_2 is computed as the total force, in the y direction, that the grains on one side of the line exert on the grains at the other side divided by the distance between the walls. The whole procedure was described elsewhere [10]. An insightful macroscopic description of the loading or unloading process can be obtained from the Mohr circle of the granular pile. In this representation, the normal and shear components applied instantaneously to every plane in the material are described as a result of the uniaxial stress. Unlike most laboratory tests, the lateral stress is not fixed, so the dynamics of both principal stresses are monitored simultaneously. The intersection of the circles with the horizontal axis represents the main stress eigenvalues, the largest σ_1, in the uniaxial direction and the smallest σ_2. Figure 2 on the right panel depicts two angles. φ_M is the internal effective friction angle as derived from the tangent to the Mohr circles. On the other hand, β is the angle between the plane depicted in the left panel and the uniaxial strain direction.

A series of Mohr circles is shown in Fig. 4 for a local friction coefficient of μ_m=0.3 as a function of the uniaxial strain. The innermost circle sequence represents the first loading cycle after the sample has been concocted, while the following two sequences correspond, monotonously, to the next two loading sequences. From the third or fourth loading cycle on, the sample achieves a stable limit and the slope of the circle sequence is computed. Such slope is taken as the macroscopic friction of the granular pack [12] and yields a precise angle φ_M of internal friction at sufficiently large stresses [12,13]. Luding [12] reported taking the correct values of friction by following the yielding circles. In our simulations, for the stable limit sequence, such yield circles fall on the same set of limiting circles.

The macroscopic friction coefficient implied by the Mohr circle sequence in Fig. 4 is μ_M=0.4 (slope joining Mohr circles), larger than the microscopic one, set here at μ_m =0.3 for grain-grain interactions. This fact is expected on general grounds since the dilatancy of the material is of structural origin and has to be taken into account in the Coulomb criterion. Such effect should require an additional apparent frictional effect, lumped into the coefficient μ_M [12]. Nevertheless, the force texture in a granular material is preparation dependent and a drastic change in the structure should change the macroscopic friction coefficient of the sample. Such force texture is readily available in our simulations and can be used to evaluate Eq. (5).

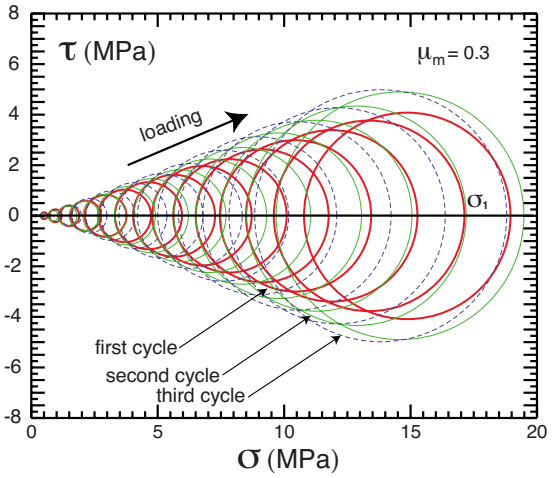

FIG. 4. (Color online) The Mohr circles as a function of the loading for three separate and consecutive cycles that go from the innermost to the outermost sequence. The vertical axis is the tangential stress applied to a plane at an angle of 2β (see Fig. 2) from the main principal axis σ_1. σ_2 is drawn as the lateral principal value at the opposite intersection of the circle with the horizontal axis. As loading increases, both σ_1 and σ_2 increase, generating a new circle. Circles in each sequence share a common tangent beyond a small loading.

The normalized frequency distribution of forces derived for the cycled granular pack at μ_m is depicted in Fig. 5. It has a symmetric twin-peaked structure with a minimum at zero and at the extreme angles $\pm\pi/2$. The shaded area indicates the physical integration range according to Eq. (5) where the upper limit is given by $\varphi_m+\pi/4$. The lower limit of the shaded region is found by fitting to the theoretical curve to the full curve of observed μ_M values found directly from the Mohr circles. Figure 6 shows a comparison between the theoretical relation involving Eq. (5) and the macroscopic friction angle measured using the Mohr circles. The fitted value for the lower angle of integration is $\phi_{min}=-0.63<-\pi/6=-0.5236\ldots$, expected as discussed above. Loading the sample changes the texture distribution somewhat in the range of loading considered (see Fig. 4) by slightly filling in

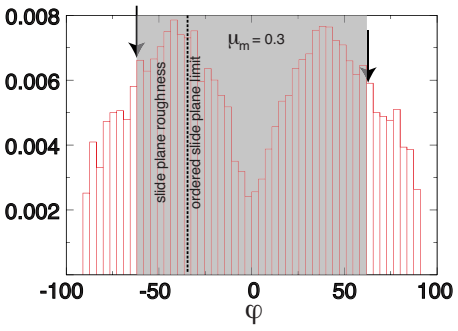

FIG. 5. (Color online) Physical integration range (gray area delimited by arrows) of the angle with respect to the vertical axis as depicted in Fig. 2. Data are directly extracted from the force orientations. Dotted line denotes the ordered plane lower-angle limit. Additional gray between this line and the left arrow is the added range generated by a roughened slide plane.

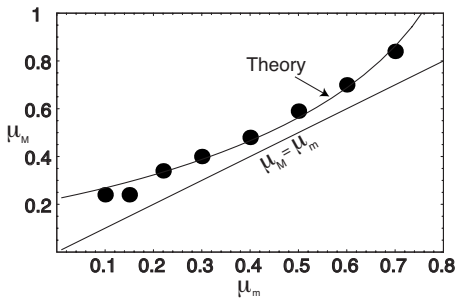

FIG. 6. Computed values of macroscopic friction (black circles) for samples with varying microscopic friction values. Error bars are of the size of the symbols. The macroscopic friction is also derived from the relation in Eq. (5) and fitted to data by adjusting one parameter describing the roughness of the sliding plane.

the valleys and reducing the peak height. Notwithstanding, such changes affect the theoretical macroscopic friction coefficient depicted in Fig. 6 less than 10% within the loading range considered.

Summarizing, we have analyzed a simple relation between local and macroscopic frictions in a two-dimensional granular pile built by deposition under the effects of gravity. The model contains the distribution of force angles in the sample, the magnitude of the local friction coefficient, and their relation to the macroscopic force on any particular plane. Macroscopic friction is defined by the sequence of Mohr yielding circles generated under increasing uniaxial strain. The results obtained are in good correspondence with the theoretical formulation analyzed for an ample range of local friction coefficients ($0.1 < \mu_m < 0.7$). Thus, the local friction plus the orientation distribution of local forces can predict macro friction behavior with only one adjustable parameter describing the roughness of the slip planes in the granular material. Even though here the macroscopic friction is always found to be larger than the local value, this depends critically on how the granular pile is built (distribution of force orientations) and a crossing between macro and local frictions can be expected, resulting in interesting stability considerations for granular piles.

This work was supported by the IVIC Rocks project and by POLAR enterprises through a LOCTI grant.

[1] M. Sadd, *Elasticity: Theory, Applications, and Numerics* (Elsevier Butterworth-Heinemann Publications, Oxford, 2005).
[2] Y. Jiang and M. Liu, Phys. Rev. Lett. **91**, 144301 (2003).
[3] J. C. Jaeger, N. G. W. Cook, and R. W. Zimmerman, *Fundamentals of Rock Mechanics*, 4th ed. (Blackwell Publishing, Oxford, 2007).
[4] J. H. Atkinson, Geotechnique **50**, 487 (2000); *Constitutive Relations of Soils*, edited by G. Gudehus, F. Darve, and I. Vardoulakis (Balkema, Rotterdam, 1984).
[5] W. Eber, Phys. Rev. E **69**, 021303 (2004).
[6] B. Cambou, Ph. Dubujet, and C. Nouguier-Lehon, Mech. Mater. **36**, 1185 (2004).
[7] J. A. Astrom, H. J. Herrmann, and J. Timonen, Phys. Rev. Lett. **84**, 638 (2000).
[8] H. A. Makse, N. Gland, D. L. Johnson, and L. M. Schwartz, Phys. Rev. Lett. **83**, 5070 (1999).
[9] J. Schäfer, S. Dippel, and D. E. Wolf, J. Phys. I **6**, 5 (1996).
[10] X. García and E. A. Medina, Geophysics **71**, F13 (2006).
[11] X. García, M. Araujo, and E. Medina, Waves Random Media **14**, 129 (2004); L. Brendel and S. Dippel, *Lasting Contacts in Molecular Dynamics Simulations*, in Physics of Dry Granular Media, edited by H. J. Herrmann, J. P. Hovi, and S. Luding (Kluwer, Dordrecht, 1998).
[12] S. Luding, J. Phys.: Condens. Matter **17**, S2623 (2005).
[13] X. García and E. Medina, Phys. Rev. E **78**, 021305 (2008).